Author's Accepted Manuscript

Stick-Slip Friction: A Monte Carlo Study

Víctor A. Bustos, Octavio J. Furlong
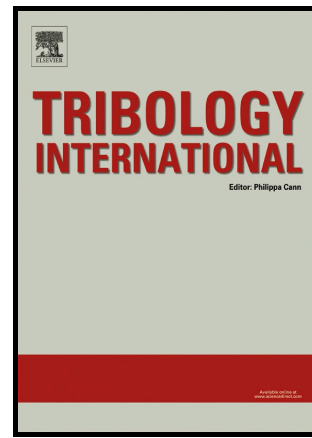
Cite this article as: Víctor A. Bustos and Octavio J. Furlong, Stick-Slip Friction: A Monte Carlo Study, *Tribiology International,* http://dx.doi.org/10.1016/j.triboint.2016.06.002

Stick-Slip Friction: A Monte Carlo Study

Víctor A. Bustos[*] and Octavio J. Furlong

INFAP/CONICET, Universidad Nacional de San Luis, Ejército de los Andes 950, 5700 San Luis, Argentina

The aim of this study is to analyze the underling molecular mechanics of the stick-slip phenomenon in confined thin films, and its dependence on parameters such as sliding velocity, load, time and temperature. The study was carried out using the kinetic Monte Carlo method, where adhesion hysteresis was explicitly introduced in a one-dimensional simulation model. A dual-interaction potential model was implemented to carry out this work. The results indicate: (i) the importance of adhesion hysteresis to explain the increase in stick-slip frequency (therefore, in sliding velocity); (ii) a consistent dependence behavior of friction in the stick-slip regime with sliding velocity, load, time and temperature; and (iii) a relationship between sliding velocity and static friction of $V_{Sliding} \propto 1/F_{Static}$.

Keywords: Stick-Slip; Adhesion hysteresis; Static friction; Monte Carlo.

*Corresponding Author: vabustos1@gmail.com

1. INTRODUCTION

Stick-slip (SS) in the boundary lubrication (BL) regime is a very important phenomenon from both technological and industrial points of view, due to that, in this regime, higher energy consumption and an increased wear of the contacting surfaces are observed [1]. With the advent of the Atomic Force Microscope (AFM) [2], the Surface Force Apparatus (SFA) [3,4] and the Quartz Crystal Microbalance (QCM) [5], it has been possible to explore the underlying physical mechanisms at the molecular level. A lot of research has been focused in the understanding of friction of systems involving confined thin films, which are of great importance in applications such as boundary lubricated engineering components, biological interfaces and microelectromechanical systems (MEMS). In particular, this type of systems have been extensively studied through SFA experiments by Israelachvilli, who, among other things, found that friction at the nano-scale could be correlated with the adhesion hysteresis phenomenon [6]. Furthermore, in order to achieve a fundamental understanding of these processes, efforts have and are still been made from both experimental [7-15] as well as theoretical and simulations points of view, such as through Molecular Dynamic Simulations (MDS) [16-28]. However, a satisfactory explanation of the friction mechanisms involved in this type of systems is still lacking, for example, with respect to the origin of phase transitions evidenced by the SS behavior and the effects of the adhesion hysteresis phenomenon.

In this contribution, the SS friction of a very thin film of simple molecules confined between two molecularly smooth surfaces, is studied by analyzing the behavior of a sample particle (SP) from the first monolayer (monolayer M) that is

susceptible to sliding due to the action of an external force (see Figure 1), by means of the kinetic Monte Carlo method.

The proposed model takes into account displacements of the confined film normal to the sliding contact, and allows to propose an explanation of the variations in thickness of the film during the development of the SS process, as well as phase transitions and oscillatory variations of the gap distance between the surfaces [21]. Also, by considering an incomplete dissipation of the energy delivered to the system by the action of an external force, an adhesion hysteresis phenomenon is introduced and its effects on the frictional behavior can be analyzed. The main objective of this work is to analyze the behavior of friction with some system parameters, and not to rigorously calculate the intrinsic friction value. The behaviors of friction with load, sliding velocity, temperature and time, previously reported by MDS and experimental results, are qualitatively reproduced by the model proposed in the present work.

2. MODEL AND METHODS

Before presenting the proposed model, some interpretations of the stick-slip type of behavior experimentally observed at sliding interfaces should be mentioned: (i) static friction is related to the "stick" event while dynamic friction to the "slip" event; (ii) thus, the stick-slip behavior is a consequence of the presence of static friction that "refuses to disappear"; (iii) it is considered that the subsequent sticks have the same molecular origin as the first one; (iv) the system starts to slide after the stick event and stops right at the end of the slip event; (v) static friction refers to the friction produced during the stick events.

It has been proposed that static friction has its origins in a monolayer of particles of a film that is in direct contact with the sliding interface [18-20, 26, 28]. The present model is based on this idea, and a basic mechanism for the study of the static friction is proposed. Furthermore, it has been shown that the friction force is linearly proportional to the number of particles that interact across the contact [29]; therefore, for a certain fixed surface density of a full monolayer, the frictional behavior has been, in the present work, analyzed by studying the average behavior of a single particle (SP). If an external force is applied to the slider (see Figure 1), it will be transmitted to the monolayer M through the upper layers of the film, probably due to a delicate balance between particle-substrate adhesion and cohesion forces within the film in the *solidlike* state. Therefore, the particles of monolayer M will be subjected to an indirect force that performs work on each particle.

The friction phenomenon under BL conditions has been analyzed through processes occurring at the lubricant-substrate interface of a confined film, and has been related to the surface physicochemistry [30]. In the present model, the stick events have been interpreted as molecular desorption processes from an initial absorbed state involving a displacement of the SP normal to the sliding contact, and the slip event as molecular migrations-adsorption processes. The desorption processes occur due to that the particle absorbs energy from an external source, which in this work is considered as a fundamental condition for the stick event to take place. The slips take place when the particle "sees" a free adsorptive neighboring site, which is a convenient place to move to and reduce its energy. In this case, the particle migrates and bounds to the new site dissipating energy. This is consistent with reports that suggest that the energy dissipation of the system mainly

occurs in the slip event [27]. Consequently, migration and adsorption events of the particle are known to be much faster than the stick events, which is in accordance with experimental results [6]; therefore, the slip events are considered to take place instantaneously right after the stick events.

There are experiments that show a dependence of the friction force with adhesion hysteresis, and that adhesion hysteresis is present regardless of the normal load values [10]; however, the effect of the presence of adhesion hysteresis during SS friction has not been tested. In addition, it is admitted that memory effects associated with the surface-film interaction are present [6]. For the simulations performed in this work, it is considered that the interactions at the substrate-film interface take place under solid-*solidlike* conditions during the stick event. A dual interaction potential that follows the principles of energy absorption/dissipation present in a Prandtl/Tomlinson-type model [31, 32], has been developed in order to be applicable to this case, where the force experienced by the SP has different characteristics than the typical elastic driving force taken into account in the classical Prandtl/Tomlinson model, as it will be describe below. The SP is initially in a bound state under a "periodic" potential and subjected to a constant indirect applied external force, where the next nearest neighbors interactions within the monolayer M have been neglected. Due to the anisotropy of the medium, it is reasonable to consider that the external force on the SP can be decomposed into two mutually orthogonal components, one parallel and one perpendicular to the sliding plane. This perpendicular component is the one pulls the SP away from the sliding contact, and is calculated in this work to obtain the static friction.

In order to calculate this static friction, it is necessary to evaluate the changes in binding energy experienced by the particle during SS. Initially, the SP is at position r_0, which is at the bottom of the binding potential, U, in its initial attractive base state, where $U(r_0, t_0) = U_0$ (see Figure 2) and is always negative (note that at an initial time t_0, $U(r_0) = U(r_1) = U(r_n)$; then, the SP starts absorbing energy as the stick event takes place; this energy is partially dissipated during the subsequent slip event, so that the binding energy of the SP at position $r_1 = r_0 + a$ and time t_1 is given by

$$U(r_1, t_1) = U(r_0, t_0) + \varepsilon U_{abs}(r_0, t'_0) \tag{1}$$

where a represents the jump length of a stick-slip event, reflecting the periodic nature of the SP interaction potential; $U_{abs}(r_0, t'_0)$ is the total energy absorbed by the particle to overcome the corresponding binding energy at time t'_0 (with $t_1 > t'_0 > t_0$), and ε is a random dimensionless parameter that represents the fraction of energy accumulated during the stick event that is not dissipated during the slip event ($\varepsilon U_{abs}(r_0, t'_0)$); this variation in the binding potential is considered as an adhesion hysteresis effect, due to that the binding energy of a certain absorbed state is higher than the corresponding subsequent state. Figure 2 shows a schematic representation of the model, showing the variations in binding potential at each position r_n, where the straight line under the particle is just a guide to show the variation of the SP base states during sliding, due to the undissipated energy. Note that r is a discrete position variable.

The general expression for the energy when the particle is at site n ($n>0$) at time t_n, with $r_n = r_{n-1} + a$, is given by

$$U(r_n, t_n) = U(r_{n-1}, t_{n-1}) + \varepsilon U_{abs}(r_{n-1}, t'_{n-1}) \qquad (2)$$

Here, the increase in energy experienced by the SP due to the work of the external force is linear with t (Equation 3). Therefore, the total energy absorbed by the SP during the stick event in the interval $(t'_n - t_n)$, is given by

$$U_{abs}(r_n, t'_n) = \alpha(t'_n - t_n) \qquad (3)$$

where α represents the rate at which the SP adsorbs energy (power) due to the action of the external force; thus, it is expressed in units of energy/time, and

$$t'_n = t_n + \sum_{i=1}^{Q}(\Delta t_n)_i \qquad (4)$$

where $(\Delta t_n)_i$ is the temporal step between successive unsuccessful transition attempts, during which the particle is absorbing energy; and Q is the number of attempts actually needed for the particle to be released. Furthermore, it is assumed that about 5 to 10 percent of the absorbed energy is not dissipated, and therefore, accumulated by the SP due to the adhesion hysteresis phenomenon, decreasing its binding energy in the subsequent absorbed state.

In order for the model to be able to consider the thermal variations during the SS on the static friction, it can be assumed that the local temperature at the interface increases due to the energy accumulated by the particle. To analyze tthis effect, a linear dependence is proposed as:

$$\Delta T = \rho \frac{\Delta U_{nd}}{k_B} \qquad (5)$$

where ρ is a dimensionless parameter that controls the temperature changes due to the amount of undissipated energy $\Delta U_{nd} = \varepsilon U_{abs}$, and k_B is the Boltzmann constant. On this basis, the temperature will increase as:

$$T = T_0 + \frac{\rho}{k_B}\sum_i(\Delta U_{nd})_i \qquad (6)$$

where T_0 is the initial temperature at time t_0, and the second term is the temperature increase of the *ith*-slip event. The sum is carried out over all the slips performed. The conversion between Monte Carlo time and real time is made by defining an elementary transition probability per unit time [33, 34]. This has been previosly used to succesfully analyze friction phenomena using the Kinetic Monte Carlo method [35-37].

The following expression can be chosen to evaluate the transition rate of the particle:

$$W_{ij}(r,t) = v e^{-\frac{\Delta E_a(r,t)}{k_B T}} \tag{7}$$

where W_{ij} is the elemental rate for the particle to go from state "i" to "j", note that backward transitions have been neglected; v is a characteristic attempt frequency of the confined particle; and $\Delta E_a(r,t)$ is the energy that the particle has to overcome to be released from its current position r_n, and is given by

$$\Delta E_a(r_n, t'_n) = -[U(r_0, t_0) - U(r_n, t'_n)] \tag{8}$$

The average force perpendicular to the surface $\left(\vec{F}_\perp \right)$ acting on the particle during each stick event is calculated considering the following expression:

$$\vec{F}_\perp . \overrightarrow{\Delta d} = \Delta U(d) \tag{9}$$

where $\Delta U(d)$ represents the change in energy during the stick event (absorbed energy) of the particle at (r_n, t'_n), and the vector $\overrightarrow{\Delta d}$ depicts the consequent change in position of the particle perpendicular to the surface (departing from the surface), which is in the same direction as $\vec{F}_\perp$. In order to calculate $\overrightarrow{\Delta d}$, we consider the attractive particle-substrate interaction potential given by Israelachvili [38]:

$$U(d) = -\frac{\pi}{6}\frac{\delta C}{d^3} \tag{10}$$

where δ corresponds to the substrate particle number density (assuming an atomic radius of $\sim$0.2 nm, $\delta = 3.0\times10^{28}$ particles/m^3); $C(\approx \sigma^6 U_0)$ is the energy coefficient, where σ is the distance at which the potential changes sign (taken equal to 0.5 nm [20]); and d is the particle-substrate distance. Here, Eq. (10) is evaluated for $U(r_n, t_n)$ and $U(r_n, t'_n)$ to obtain $\overrightarrow{\Delta d}$. Note that the magnitude of $\Delta U(d)$ (see Eq. 9) is equal to $U_{abs}(r_n, t'_n)$, so that the magnitude of $\vec{F}_\perp$ for each stick is given by:

$$F_\perp = \frac{U_{abs}(r_n, t'_n)}{\Delta d} \tag{11}$$

This expression basically describes the adhesion force that gives rise to the friction force during the stick event, so we will refer to this force as static friction [28]. For simulation practical purposes, the average static friction is calculated from the values of N sticks ($N = 6$ was used in the calculations). The energy traces were repeated u times (with $u = 10^3$) in statistically independent processes. Then,

$$\langle F_{static}(r, t) \rangle = \frac{1}{u}\sum_{i=1}^{u} \langle F_\perp{}^i \rangle_{Nsticks} \tag{12}$$

The sliding velocity of the particle is easily obtained since a travel distance "a" is associated to each SS event, and the elapsed time is obtained from the simulation. The average sliding velocity is calculated over N sticks-slip events ($N = 6$), and then averaged out over u energy traces.

3. RESULTS AND DISCUSSION

All the calculations were performed with $v = 10^6$ s^{-1} and ε being a random parameter with values of $0.05 \leq \varepsilon \leq 0.10$; the distance between sites "a" was taken equal to 0.6 nm, and a value of 1 meV/s was chosen for the parameter α. Note that no reduced variables or fitting parameters have been used. The size of the

points in the figures reflects an over-estimation of the statistical error in the calculated magnitudes; the lines connecting points are just a guide to the eye.

The changes in temperature resulting from the fraction of undissipated energy (Equation 5) during the number of SS events performed are very small compared to the initial temperatures used in this work, and do not have a significant effect on the static friction behavior (data not shown); thus, the results shown were obtained for $\rho = 0$ (constant temperature). Nevertheless, results were obtained for different constant temperatures.

Shown in Figure 3 is the change in the SP binding energy as a function of time (energy traces) at $T = 290$ K. The same temporal range of 150 seconds is plotted for different initial binding potentials, U_0 (20, 30 and 40 meV [20]). Note that, in our model, the change in U_0 (binding energy or transition energy barrier) could be also interpreted as a change in normal load [39, 40]. It can be observed that the SS frequency decreases with U_0 (or normal load), therefore resulting in a decrease in sliding velocity, which is accompanied by an increase of friction (see Figure 4); this behavior has been observed during friction trace experiments (see Fig. 10(a) from Ref. [6]), thus corroborating this interpretation of the relationship between U_0 and the normal load. Also note that, in all cases, the resulting binding energy decreases with time as a consequence of the fraction of undissipated energy; this effect can be considered as an adhesion hysteresis phenomenon, since the energy required to desorb the SP particle from certain state is higher than the binding energy of the subsequent state.

Figure 4 shows the static friction versus the binding potential, U_0, at a temperature of 290 K. These results are in qualitatively agreement with previous

experimental results (see figure inset, [6]), and show that the behavior of the static friction is linear with respect to the normal load. This corroborates even further the mentioned assumption in the relationship between U_0 and normal load, especially when a constant friction coefficient is assumed.

Figure 5 shows the sliding velocity versus binding potential, where the plotted points correspond to the average sliding velocity obtained for the first 6 SS events. This type of behavior has also been observed in experimental results (see Fig. 13(a) from Ref. [6]). Note that, according to Figure 4, the x-axis can be easily converted into values of static friction; then, plotting sliding velocity versus $1/F_{static}$ (inset, Figure 5), it can be observed that this relationship follows a $V_{sliding} \propto 1/F_{static}$ dependence (note that the proportionality factor is not perfectly constant).

Figure 6 shows the static friction versus time, where it can be observed that the static friction decreases with time, which in this model, is due to the accumulation of undissipated energy as sliding takes place (adhesion hysteresis effect). The same behavior has been observed in experimental results for a confined film of complex molecules (see inset) [8]. Note that under complete energy dissipation ($\varepsilon = 0$ or no adhesion hysteresis effect), friction would remain constant with time.

From the above, when adhesion hysteresis effects are taken into account, a decrease of the friction force with time is observed and, at the same, according to Figure 5, there should be an increase of the sliding velocity as the friction force decreases. This is observed in Figure 7, which shows the results of static friction versus sliding velocity for $U_0 = 30$ meV and $T = 290$ K, when adhesion hysteresis effects are taken into account. Clearly, static friction decreases with the sliding

velocity following once again a relationship of the type $V \propto 1/F$ (see inset). It is worth mentioning that the curves obtained for other values of U_0 and T show the same behavior (data not shown).

Finally, Figure 8 shows results of static friction at different temperatures for different binding potentials U_0 (20, 30 and 40 meV), where a linear decrease of static friction with temperature is observed, in agreement with MDS results (see Fig. 5 from Ref. [20]) and experimental results (see Fig. 4 from Ref. [13]). Note that this is consistent with the expected behavior of a thermally activated process.

In addition, the present model allows to speculate about the SS phase transitions of simple molecules. Based on the results obtained by Schoen et al. [40, 41] that show that the gap between the surfaces determines the state of order or disorder of a confined thin film, a molecular mechanism that could lead to SS phase transitions is suggested in the following.

3.1 SS order-disorder dynamic transitions

Let us consider that an adsorbed molecule moves away from the surface when it is mechanically activated by effect of the external force, thus weakening its binding energy [43]. In order to better understand this interpretation, from a simplified point view, we can think of a hard sphere-type film, and then take into account the entire M monolayer instead of just one particle. Now, we can consider that the phenomenon begins with the film in an ordered *solidlike* state, confined within an initial gap D_0. When the monolayer M is activated, it is forced to depart from the substrate colliding with particles of the monolayer immediately above, and so on up to the upper layers of the film. Consequently, repulsive forces emerge producing instabilities in the initial ordered state of the film generating a temporary

disorder (*liquidlike* state), and thus slightly increasing the corresponding gap. Subsequently, and probably by effect of the parallel external force, the disordered particles migrate until they find the appropriate situation to reduce the energy of the system. Thus, the activated particles from the M monolayer find an empty neighboring site to bind once again, "approaching" the substrate and dissipating a great proportion of their energy. Note that the particles of the M monolayer are indistinguishable for the substrate. Consequently, the ordered *solidlike* state is recovered and the gap decreases once again, although not to its initial value, but to a slightly higher gap distance, due to the hysteresis phenomenon. Note that this film order-disorder sequence is repeated as the SS progresses.

3.2 SS to smooth sliding

In accordance to the expressed above, a qualitative interpretation of the first order transition from SS to smooth sliding that have been experimentally observed [6] may be also proposed. It is assumed that, due to hysteresis effects, the M monolayer departs from the substrate as time evolves, until reaching a maximum departing distance at a time referred to as critical time, at which the particles remain under a disordered state. From the kinetic Monte Carlo simulations, it is found that the average maximum departing distance is some tenths of nanometers. It should be noted that after this critical time, the thermal impulses are sufficient to continuously overcome the residual binding energies, leading to continuous sliding. Therefore, at this point, the system has reached a steady state of higher energy, where the particles of the M monolayer are practically free from the substrate, and the film is found and remains in a *liquidlike* state, leading to smooth sliding, where the system slides under dynamic friction conditions.

4. CONCLUSIONS

Apparently, the static friction refuses to disappear when two surfaces start a relative motion under boundary lubrication conditions, giving rise to the SS phenomenon. In order to study the SS phenomena in sliding systems involving confined thin film, a dual interaction potential model was developed and implemented, by means of the kinetic Monte Carlo method. On one hand, the model takes into account displacements of the confined film normal to the sliding contact, and on the other hand, it considers the effects of an incomplete dissipation of the energy which can be interpreted as an adhesion hysteresis phenomenon.

The obtained static friction results are qualitatively consistent with previous experiments and MDS results. The adhesion hysteresis phenomenon in static friction, according to the interpretation of the presented model, is of fundamental relevance in the frictional behavior of the system. Here, the static friction value is directly related to the work performed by the external force applied that brakes the ordered state of the film during each SS transition. Furthermore, due to an incomplete energy dissipation, the system reaches a higher-energy state, leading to a decrease in the static friction (the spike amplitude decreases) as the SS evolves over time. Consequently, an increase in the SS frequency is found, which is compatible with the increase observed in sliding velocity. A relationship between the sliding velocity of the system and the observed static friction was found, where $V_{sliding} \alpha 1/ F_{Static}$.

This model allows to speculate that there are at least two types of forces present in the friction traces. On one hand, static friction, which is directly related to

the *solidlike* state of the film due to the relatively strong interactions between the substrate and the monolayer M (mainly chemical forces). On the other hand, dynamic friction, which is related to a *liquidlike* state of the film, is mainly due to the inter-particle interactions in the film (mainly physical forces). It is known that transient changes in the film thickness during the SS produce changes in its density [44, 45]. This can now be understood by considering that the M monolayer moves slightly away from the substrate, pushing up the layers of the film; therefore, momentarily reducing the film thickness during a SS transition. This consideration also allows to explain the oscillatory changes of the slider-substrate distance that have been experimentally observed [21]. Finally, according to this model, the absorption (stick) and dissipation (slip) of energy could be thought as a molecular picture responsible for the energy pump of the system.

5. ACKNOWLEDGEMENTS

6. REFERENCES

[1] B. N. J. Persson, Surf.Sc. Rep. **33**, 83-119(1999).
[2] G. Binning, C. F. Quate and Ch. Gerber, Phys. Rev. Lett. **56**, 930 (1986).
[3] D. Tabor, R. Winterton, Proc. R. Soc. London A **312**, 435 (1969).
[4] J. N. Israelachvili, D. Tabor, Proc. R. Soc. London A **331**, 19 (1972).
[5] J. Krim and A. Widom, Phys. Rev. B **38**(17), 12184 (1988).
[6] H. Yoshizawa and J. N. Israelachvili, J. Phys. Chem. **97**, 11300 (1993).
[7] G. Jianping, W. D. Luedfke, D. Gourdon, M. Ruths, J. N. Israelachvili and U. Landman, J. Phys. Chem. B **108**, 3410 (2004).
[8] C. Drummond and J. N. Israelachvili, Macromolecules **33**, 4910 (2000).

[9] I. Krupka, M. Hartl and M. Liska, Tribol. Int. **39**, 1726 (2006).

[10] H. Yoshizawa, Y. Chen and J. N. Israelachvili, J. Phys. Chem. **97**, 4128 (1993).

[11] S. Itoh, K. Ishii, K. Fukuzawa and H. Zhang, Tribol. Lett. **53**, 555 (2014).

[12] I. S. Y. Ku, W.W. F. Chong, T. Reddyhoff and H. Rahnejat, Meccanica **55**, 1915 (2015).

[13] M. He, A. Szuchmacher Blum, G. Overney and R. M. Overney, Phys. Rev. Lett. **88**(15), 154302 (2002).

[14] M. Ruths, N. A. Alcantar and J. N. Israelchvili, J. Phys. Chem. B **107**, 11149 (2003).

[15] C. Drummond and J. N. Israelachvili, Phys. Rev. E **63**, 041506 (2001).

[16] Y. Lei and Y. Leng, Phys. Rev. Lett. **107**, 147801 (2011).

[17] A. Jabbarzadeh, Tribol. Int. **97**, 108 (2016).

[18] B. N. J. Persson, J. Chem. Phys. **103**, 3849 (1995).

[19] M. H. Muser and M. O. Robbins, Science **284**, 1650 (1999).

[20] G. He and M. O. Robbins, Phys. *Rev. B* **64**, 035413 (2001).

[21] P. A. Thompson and M. O. Robbins, Science **250**, 792 (1990).

[22] I. M. Sivebaek, B. N. J. Persson, Tribol. Lett. **62**:5 (2016).

[23] C. Hu, M. Bai, J. Lv, P. Wang and X. Li, Tribol. Int. **78**, 152 (2014).

[24] B. N. J. Persson, Phys. Rev. B **55**, 8004 (1997).

[25] Y. Zhang, J. Mol. Liquid **128**, 56 (2006).

[26] B. N. J. Persson, Phys. Rev B **48**, 18140 (1993).

[27] J. Klein, Phys. Rev. Lett. **98**, 056101 (2007).

[28] Q. Zhang, Y. Qi, L. G. Hector Jr., T. Cagin, and W. A. Goddard III, Phys. Rev. **75**, 144114 (2007).

[29] Y. Mo, T. Turner and I. Szlufarska, Nature **457**, 1116 (2009).

[30] O. M. Braun and A. G. Naumovets, Surf. Sc. Rep. **60**, 79 (2006).

[31] G. A. Tomlinson, Philos. Mag. Ser. **7**(7), 905 (1929).

[32] L. Prandtl, J. App. Math. Mech. **8**, 85 (1928).

[33] K. A. Fichthorn and W. H. Weinberg, J. Chem. Phys. **95**, 1090 (1991).

[34] J. L. Sales, R. O. Uñac, M. V. Gargiulo, V. Bustos, and G. Zgrablich, Langmuir **12**, 95 (1996).

[35] O. J. Furlong, S. J. Manzi, V. D. Pereira, V. A. Bustos and W. T. Tysoe, Phys. Rev. B **80**, 153408 (2009).

[36] S. J. Manzi, W. T. Tysoe, O. J. Furlong, Tribol. Lett. **55**, 363 (2014)

[37] O. J. Furlong, S. J. Manzi, A. Martini and W. T. Tysoe, Tribol. Lett. **60**:21 (2015)

[38] J. N. Israelachvili, *Intermolecular and Surface Force*, Academic Press, London, 3rd edition (2011).

[39] E. Riedo, E. Gnecco, R. Bennewitz, E. Meyer and H. Brune, Phys. Rev. Lett. **91**, 084502 (2003).

[40]   O. J. Furlong, S. J. Manzi, V. D. Pereyra, V. Bustos and W. T. Tysoe, Tribol. Lett. **39**, 177 (2010).

[41] C. L. Rhykerd Jr., M. Schoen, D. J. Diestler and J. H. Cushman, Nature **33**, 461(1987).

[42] M. Schoen, D. J. Diestler and J. H. Cushman, J. Chem. Phys. **87**, 5464(1987).

[43] M. A. Lantz, H. J. Hug, R. Hoffmann, P. J. A. van Schendel, P. Kappenberger, S. Martin, A. Baratoff and H. J. Guntherodt, Science **291**, 2580 (2001).

[44] E. Kumacheva and J. Klein, J. Chem. Phys **108**, 7010 (1998).

[45] A. Dhinojwala, S. C. Bae and Steve Granick, Tribol. Lett. **9**, 55-62 (2000).

Figure Captions

Figure 1: Schematic representation of two surfaces with a confined thin film in between. In this case, the M monolayer is adhered to the fixed substrate and is susceptible to sliding. D_0 corresponds to the initial gap between the two surfaces.

Figure 2: Schematic representation of the particle-substrate interaction potential. The solid curves represent the binding potential (Equation 10) at the discrete positions *r*. The straight solid line represents the increase of the particle potential energy, due to the undissipated energy, as sliding occurs.

Figure 3: SP binding energy versus time. The calculations were performed at $T = $ 290 K. (A) $U_0 = 20$ meV, (B) $U_0 = 30$ meV and (C) $U_0 = 40$ meV. Note that all binding energies are negative (attractive potential).

Figure 4: Static friction versus binding potential, U_0, at $T = 290$ K. The inset shows previous experimental results of static friction versus normal loads for hexadecane thin confined films at two different temperatures [6].

Figure 5: Sliding velocity versus binding potential U_0 at $T = 290$ K. The inset shows the sliding velocity versus 1/static friction, where the conversion between binding potential and static friction is based on Figure 4.

Figure 6: Static friction versus time for two different binding potentials: $U_0 = 20$ meV (○) and $U_0 = 40$ meV (●), at $T = 290$ K. Shown in the inset are experimental results of friction force versus sliding time for confined thin films of squalene at two different normal loads [8].

Figure 7: Static friction versus sliding velocity for $U_0 = 30$ meV and $T = 290$ K, for a system with incomplete energy dissipation ($\varepsilon \neq 0$). The inset shows the same results plotted as static friction versus 1/sliding velocity.
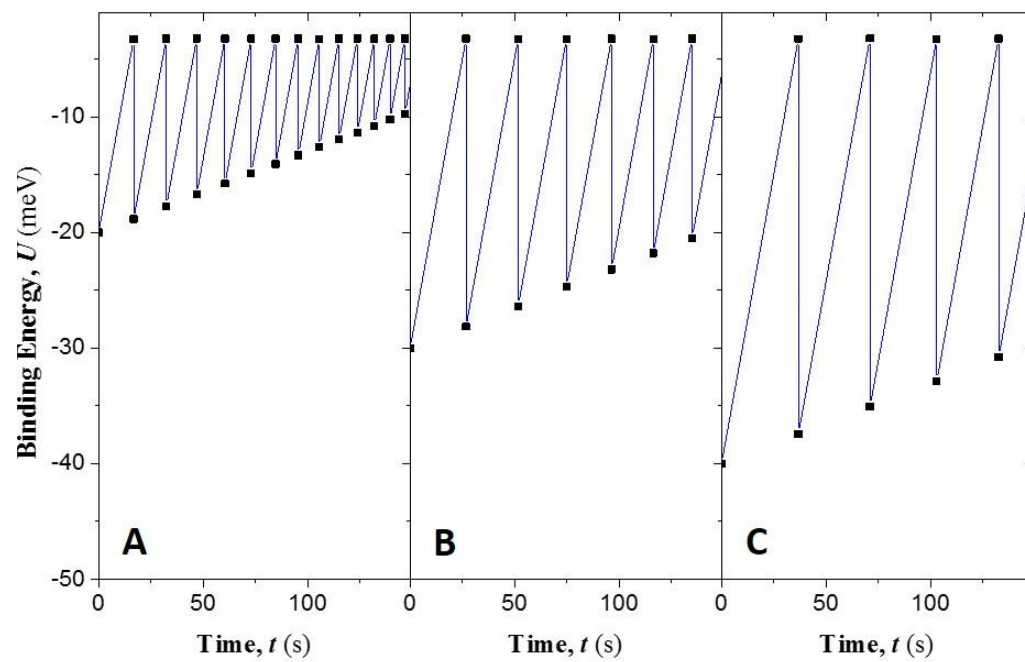
Figure 8: Static friction versus temperature for different values of the binding potential, $U_0 = 20$ meV ($\circ$), $U_0 = 30$ meV ($\bullet$) and $U_0 = 40$ meV ($\square$).
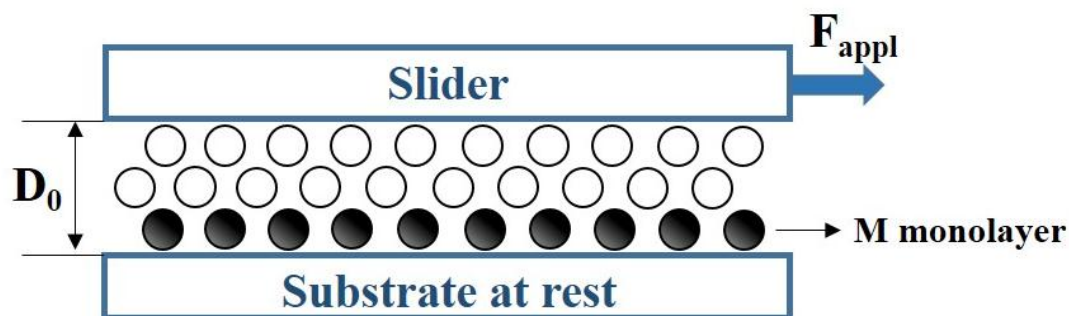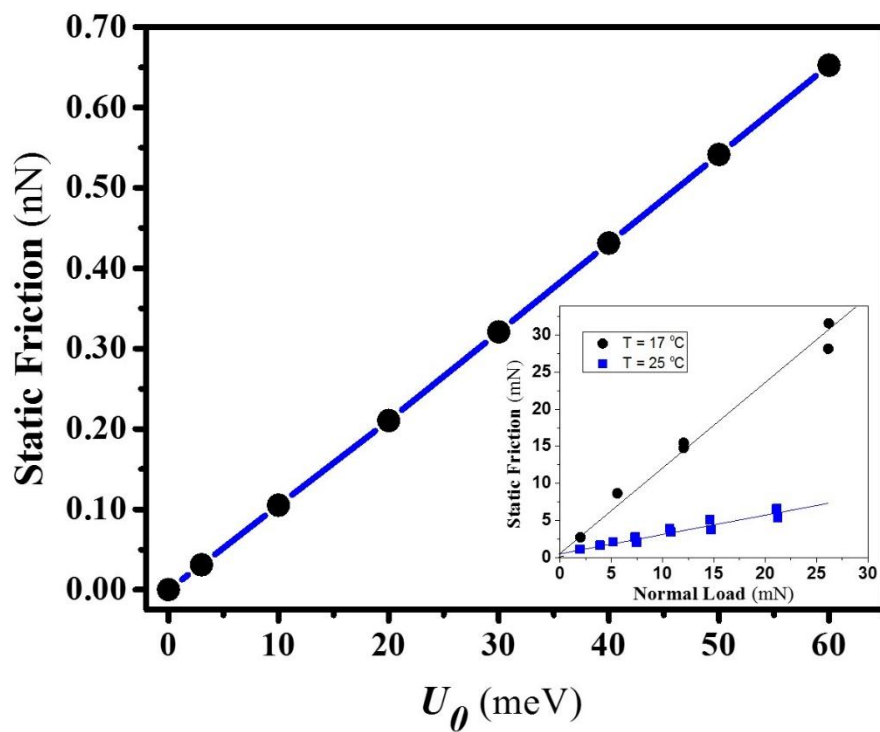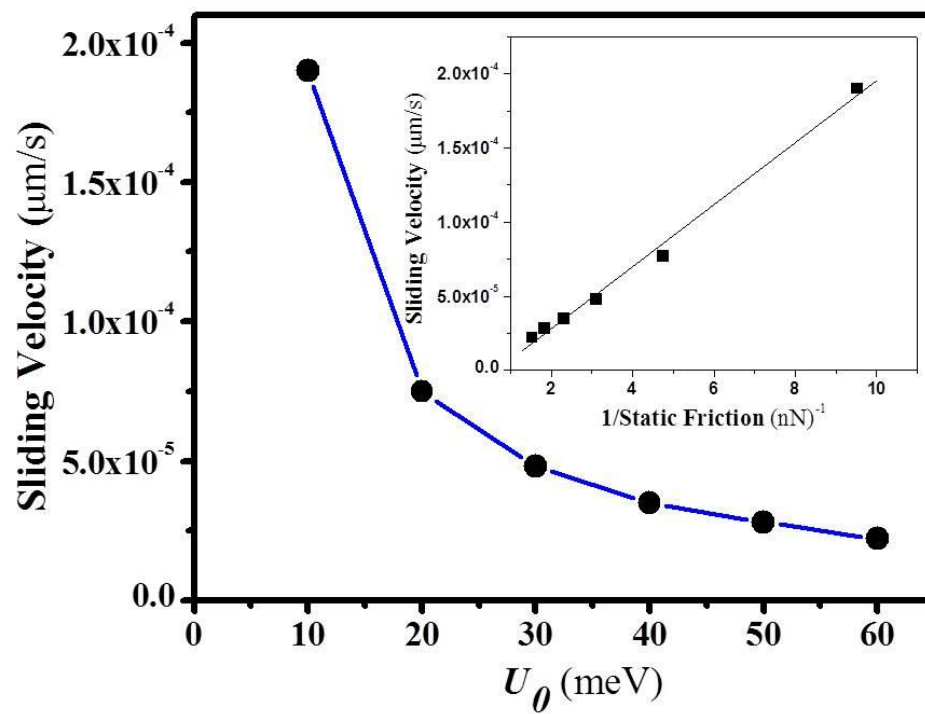

Bustos and Furlong, Figure 1
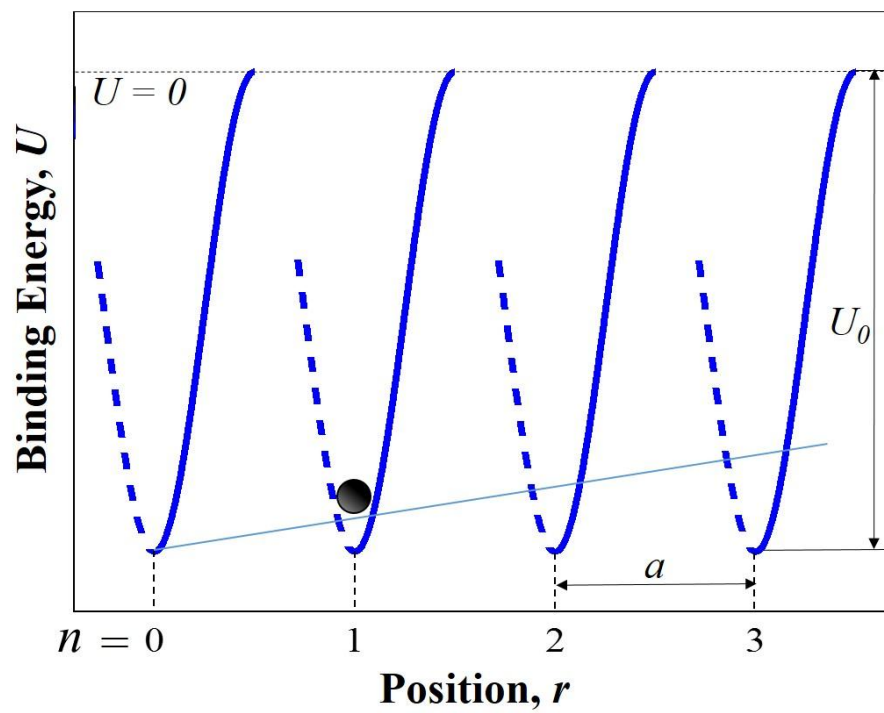
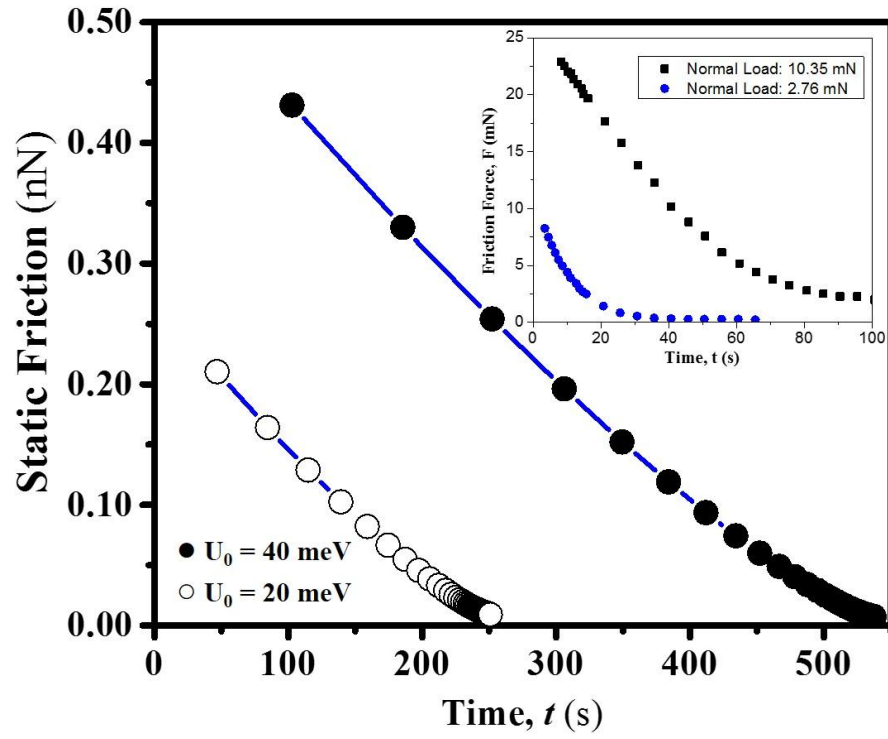*Bustos and Furlong, Figure 2*

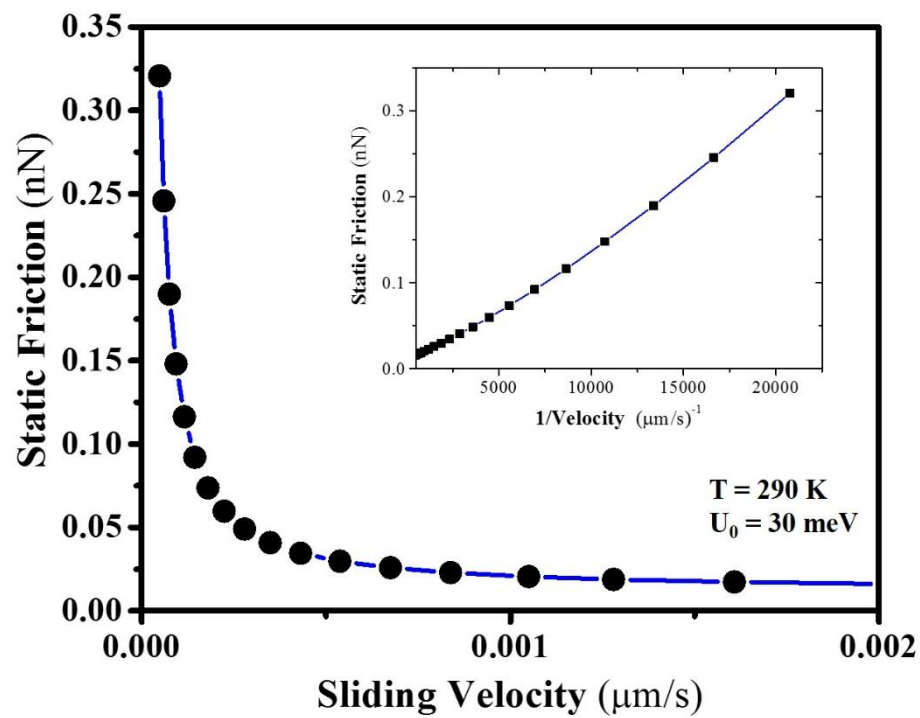*Bustos and Furlong, Figure 3*

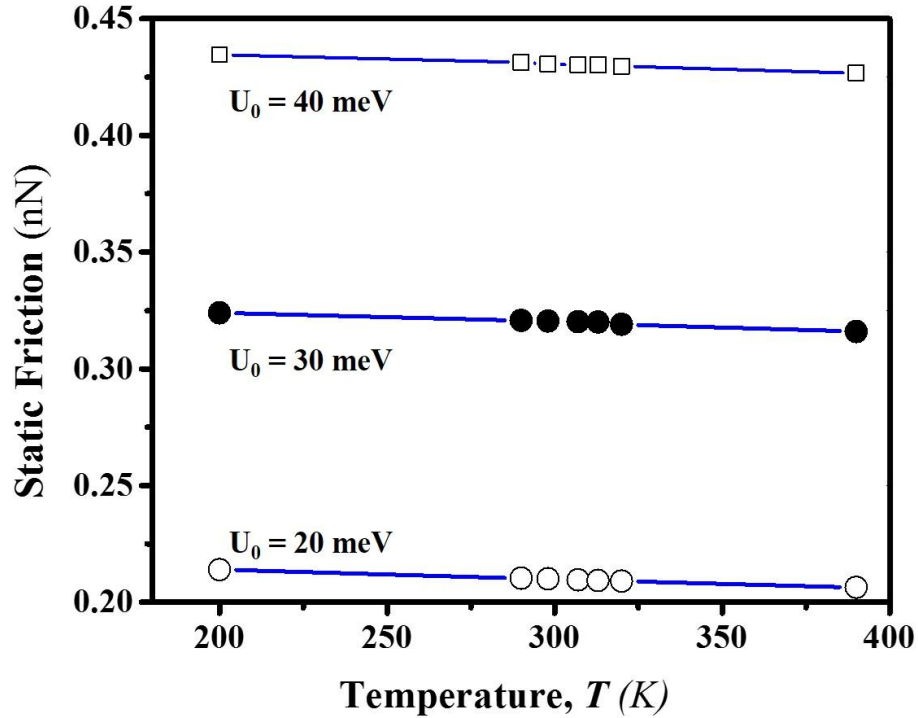*Bustos and Furlong, Figure 4*

Bustos and Furlong, Figure 5

Bustos and Furlong, Figure 6

Bustos and Furlong, Figure 7

Bustos and Furlong, Figure 8

Highlights:

- **A dual-interaction model has been applied in confined thin film lubrication**
- **The effects of incomplete energy dissipation are analyzed**
- **Sliding velocity and friction show an inversely proportional relationship**
- **A molecular interpretation of a confined film order-disorder transitions is provided**